

**Magnetic moments of the doubly charmed and bottom baryons**Hao-Song Li,<sup>1,\*</sup> Lu Meng,<sup>2,†</sup> Zhan-Wei Liu,<sup>3,‡</sup> and Shi-Lin Zhu<sup>1,4,§</sup><sup>1</sup>*School of Physics and State Key Laboratory of Nuclear Physics and Technology, Peking University, Beijing 100871, China*<sup>2</sup>*School of Physics, Peking University, Beijing 100871, China*<sup>3</sup>*School of Physical Science and Technology, Lanzhou University, Lanzhou 730000, China*<sup>4</sup>*Collaborative Innovation Center of Quantum Matter, Beijing 100871, China*

(Received 21 July 2017; published 18 October 2017)

The chiral corrections to the magnetic moments of the spin- $\frac{1}{2}$  doubly charmed baryons are systematically investigated up to next-to-next-to-leading order with heavy baryon chiral perturbation theory. The numerical results are calculated up to next-to-leading order:  $\mu_{\Xi_{cc}^{++}} = -0.25\mu_N$ ,  $\mu_{\Xi_{cc}^{+}} = 0.85\mu_N$ ,  $\mu_{\Omega_{cc}^{+}} = 0.78\mu_N$ . We also calculate the magnetic moments of the other doubly heavy baryons, including the doubly bottom baryons ( $bbq$ ) and the doubly heavy baryons containing a light quark, a charm quark, and a bottom quark ( $\{bc\}q$  and  $[bc]q$ ):  $\mu_{\Xi_{bb}^{0}} = -0.84\mu_N$ ,  $\mu_{\Xi_{bb}^{-}} = 0.26\mu_N$ ,  $\mu_{\Omega_{bb}^{-}} = 0.19\mu_N$ ,  $\mu_{\Xi_{\{bc\}q}^{+}} = -0.54\mu_N$ ,  $\mu_{\Xi_{\{bc\}q}^{0}} = 0.56\mu_N$ ,  $\mu_{\Omega_{\{bc\}q}^{0}} = 0.49\mu_N$ ,  $\mu_{\Xi_{[bc]q}^{+}} = 0.69\mu_N$ ,  $\mu_{\Xi_{[bc]q}^{0}} = -0.59\mu_N$ ,  $\mu_{\Omega_{[bc]q}^{0}} = 0.24\mu_N$ .

DOI: 10.1103/PhysRevD.96.076011

**I. INTRODUCTION**

The SELEX Collaboration first reported evidence for the doubly charmed baryon  $\Xi_{cc}^{+}(3520)$  in the decay mode  $\Xi_{cc}^{+} \rightarrow \Lambda_c^{+} K^{-} \pi^{+}$  with the mass  $M_{\Xi_{cc}^{+}} = 3519 \pm 1$  MeV [1], although other experimental collaborations—like FOCUS [2], BABAR [3], and Belle [4]—did not find any evidence of the doubly charmed baryons. Recently, the LHCb Collaboration observed  $\Xi_{cc}^{++}$  in the  $\Lambda_c^{+} K^{-} \pi^{+} \pi^{+}$  mass spectrum with the mass  $M_{\Xi_{cc}^{++}} = 3621.40 \pm 0.72(\text{stat}) \pm 0.27(\text{syst}) \pm 0.14(\Lambda_c^{+})$  MeV [5].

In the past decade, there have been many investigations of the doubly charmed baryon masses [6–40]. However, the electromagnetic form factors (especially the magnetic moments) play a pivotal role in describing the inner structures of hadrons. In the quark model, the doubly charmed baryons are just like the light baryons with two light quarks replaced by two charm quarks. The magnetic moments of doubly charmed baryons were first investigated by Lichtenberg in Ref. [41] with the nonrelativistic quark model. Since then, more elaborate quark models have been developed to study the magnetic moments of doubly charmed baryons. In Ref. [8], various static properties including magnetic moments were studied within the nonrelativistic quark model using the Faddeev formalism. Magnetic moments were also evaluated in the relativistic quark model [42,43]. In Ref. [44], the radiative decays of double heavy baryons were studied in a relativistic constituent three-quark model including hyperfine mixing.

Besides the quark models, the magnetic moments of the doubly charmed baryons have been studied with other approaches, such as the MIT bag model [45,46], the Dirac equation formalism [47], the Skyrminion model [48], the hyper central description of the three-body system [49], and lattice QCD [50,51]. In Refs. [50,51], the authors studied the electromagnetic properties of baryons in  $2 + 1$ -flavor lattice QCD. They found that the magnetic moments of the singly charmed baryons are dominantly determined by the light quarks, while the charm quarks play a more important role in the doubly charmed baryons, which is confirmed in this paper.

Unfortunately, most of the above models miss the chiral corrections. The Goldstone boson cloud effect can be taken into account through chiral perturbation theory [52], which organizes the low-energy interactions order by order. Since the baryon mass  $M$  does not vanish in the chiral limit, the convergence of the chiral expansion is destroyed by the large energy scale  $M$ . To overcome the above difficulty, heavy baryon chiral perturbation theory (HBChPT) was proposed [53–56], which has been successfully used in the investigation of baryons. For the doubly charmed baryons, the two charmed quarks are so heavy that they can be treated as spectators. Thus, the remaining light quark dominates the chiral dynamics of the doubly charmed baryons.

In this work, we will investigate the magnetic moments of the spin- $\frac{1}{2}$  doubly charmed or bottom baryons with HBChPT. Right now, there does not exist any experimental measurement of the magnetic moments of the doubly charmed baryons. We use the quark model to estimate the corresponding low-energy constants (LECs) and calculate the chiral corrections to the magnetic moments order by order. The numerical results are presented up to

\*haosongli@pku.edu.cn

†lmeng@pku.edu.cn

‡liuzhanwei@lzu.edu.cn

§zhsl@pku.edu.cn

next-to-leading order while the analytical results are calculated to next-to-next-to-leading order.

Our work is organized as follows. In Sec. II, we discuss the electromagnetic form factors of the spin- $\frac{1}{2}$  doubly charmed baryons. In Sec. III, we introduce the effective chiral Lagrangians. We calculate the chiral corrections to the magnetic moments order by order in Sec. IV and present our numerical results in Sec. V. A short summary is given in Sec. VI. We collect the coefficients of the loop corrections in the Appendix.

## II. ELECTROMAGNETIC FORM FACTORS OF SPIN- $\frac{1}{2}$ DOUBLY CHARMED BARYONS

For the spin- $\frac{1}{2}$  doubly charmed baryons, the matrix elements of the electromagnetic current are similar to that of the nucleon,

$$\langle \Psi(p') | J_\mu | \Psi(p) \rangle = e \bar{u}(p') \mathcal{O}_\mu(p', p) u(p), \quad (1)$$

with

$$\mathcal{O}_\mu(p', p) = \frac{1}{M_H} \left[ P_\mu G_E(q^2) + \frac{i\sigma_{\mu\nu} q^\nu}{2} G_M(q^2) \right], \quad (2)$$

where  $P = \frac{1}{2}(p' + p)$ ,  $q = p' - p$ , and  $M_H$  is the doubly charmed baryon mass.

As the doubly charmed baryons are very heavy compared to the chiral symmetry breaking scale, we adopt the heavy-baryon formulation. In the heavy-baryon limit, the spin- $\frac{1}{2}$  doubly charmed baryon field  $B$  can be decomposed into the large component  $H$  and the small component  $L$ ,

$$B = e^{-iM_H v \cdot x} (H + L), \quad (3)$$

$$H = e^{iM_H v \cdot x} \frac{1 + \not{v}}{2} B, \quad L = e^{iM_H v \cdot x} \frac{1 - \not{v}}{2} B, \quad (4)$$

where  $v_\mu = (1, \vec{0})$  is the velocity of the baryon. Now the doubly charmed baryon matrix elements of the electromagnetic current  $J_\mu$  read

$$\langle H(p') | J_\mu | H(p) \rangle = e \bar{u}(p') \mathcal{O}_\mu(p', p) u(p). \quad (5)$$

The tensor  $\mathcal{O}_\mu$  can be parametrized in terms of electric and magnetic form factors,

$$\mathcal{O}_\mu(p', p) = v_\mu G_E(q^2) + \frac{[S^\mu, S^\nu] q^\nu}{M_H} G_M(q^2), \quad (6)$$

where  $G_E(q^2)$  is the electric form factor and  $G_M(q^2)$  is the magnetic form factor. When  $q^2 = 0$ , we obtain the charge ( $Q$ ) and magnetic moment ( $\mu_H$ ),

$$Q = G_E(0), \quad \mu_H = \frac{e}{2M_H} G_M(0). \quad (7)$$

## III. CHIRAL LAGRANGIANS

### A. The leading-order chiral Lagrangians

To calculate the chiral corrections to the magnetic moment, we construct the relevant chiral Lagrangians. The spin- $\frac{1}{2}$  doubly charmed baryon field reads

$$\Psi = \begin{pmatrix} \Xi_{cc}^{++} \\ \Xi_{cc}^+ \\ \Omega_{cc}^+ \end{pmatrix} \Rightarrow \begin{pmatrix} ccu \\ ccd \\ ccs \end{pmatrix}. \quad (8)$$

We follow Refs. [56–58] to define the basic chiral effective Lagrangians of the pseudoscalar mesons. The pseudoscalar meson fields are introduced as follows:

$$\phi = \begin{pmatrix} \pi^0 + \frac{1}{\sqrt{3}}\eta & \sqrt{2}\pi^+ & \sqrt{2}K^+ \\ \sqrt{2}\pi^- & -\pi^0 + \frac{1}{\sqrt{3}}\eta & \sqrt{2}K^0 \\ \sqrt{2}K^- & \sqrt{2}K^0 & -\frac{2}{\sqrt{3}}\eta \end{pmatrix}. \quad (9)$$

The chiral connection and axial-vector field are defined as [56,58]

$$\Gamma_\mu = \frac{1}{2} [u^\dagger (\partial_\mu - ir_\mu) u + u (\partial_\mu - il_\mu) u^\dagger], \quad (10)$$

$$u_\mu \equiv \frac{1}{2} i [u^\dagger (\partial_\mu - ir_\mu) u - u (\partial_\mu - il_\mu) u^\dagger], \quad (11)$$

where

$$u^2 = U = \exp(i\phi/f_0), \quad (12)$$

$$r_\mu = l_\mu = -eQA_\mu. \quad (13)$$

For Lagrangians with baryon fields  $Q = Q_H = \text{diag}(2, 1, 1)$ , and for the pure meson Lagrangians  $Q = Q_m = \text{diag}(2/3, -1/3, -1/3)$ .  $f_0$  is the decay constant of the pseudoscalar meson in the chiral limit. The experimental value of the pion decay constant  $f_\pi \approx 92.4$  MeV, while  $f_K \approx 113$  MeV and  $f_\eta \approx 116$  MeV.

The leading-order [ $\mathcal{O}(p^2)$ ] pure meson Lagrangian is

$$\mathcal{L}_{\pi\pi}^{(2)} = \frac{f_0^2}{4} \text{Tr}[\nabla_\mu U (\nabla^\mu U)^\dagger], \quad (14)$$

where

$$\nabla_\mu U = \partial_\mu U - ir_\mu U + iUl_\mu. \quad (15)$$

The superscript denotes the chiral order.

The leading-order pseudoscalar meson and doubly charmed baryon interaction Lagrangians read

$$\mathcal{L}^{(1)} = \bar{\Psi}(i\not{D} - M_H)\Psi, \quad (16)$$

$$\mathcal{L}_{\text{int}}^{(1)} = \frac{\tilde{g}_A}{2} \bar{\Psi} \gamma^\mu \gamma_5 u_\mu \Psi, \quad (17)$$

where  $\mathcal{L}_0^{(1)}$  and  $\mathcal{L}_{\text{int}}^{(1)}$  are the free and interaction parts, respectively, and  $M_H$  is the doubly charmed baryon mass,

$$D_\mu \Psi = \partial_\mu \Psi + [\Gamma_\mu, \Psi]. \quad (18)$$

In the framework of HBChPT, the leading-order nonrelativistic pseudoscalar meson and doubly charmed baryon Lagrangians read

$$\mathcal{L}_0^{(1)} = \bar{H}(i\nu \cdot D)H, \quad (19)$$

$$\mathcal{L}_{\text{int}}^{(1)} = \tilde{g}_A \text{Tr} \bar{H} S^\mu u_\mu H, \quad (20)$$

where  $S_\mu = \frac{i}{2} \gamma_5 \sigma_{\mu\nu} v^\nu$  is the covariant spin operator. We do not consider the mass differences between different doubly charmed baryons. We estimate the  $\phi HH$  coupling  $\tilde{g}_A = -0.5$  with the help of the quark model in Sec. V. For the pseudoscalar meson masses, we use  $m_\pi = 0.140$  GeV,  $m_K = 0.494$  GeV, and  $m_\eta = 0.550$  GeV. We use the nucleon masses  $M_B = 0.938$  GeV.

### B. The next-to-leading-order chiral Lagrangians

The  $\mathcal{O}(p^2)$  Lagrangian contributes to the magnetic moments of the doubly charmed baryons at the tree level,

$$\mathcal{L}^{(2)} = \frac{a_1}{8M_B} \bar{\Psi} \sigma^{\mu\nu} \hat{F}_{\mu\nu}^+ \Psi + \frac{a_2}{8M_B} \bar{\Psi} \sigma^{\mu\nu} \text{Tr}(F_{\mu\nu}^+) \Psi, \quad (21)$$

where the coefficients  $a_{1,2}$  are the LECs. The chiral covariant QED field-strength tensor  $F_{\mu\nu}^\pm$  is defined as

$$F_{\mu\nu}^\pm = u^\dagger F_{\mu\nu}^R u \pm u F_{\mu\nu}^L u^\dagger, \quad (22)$$

$$F_{\mu\nu}^R = \partial_\mu r_\nu - \partial_\nu r_\mu - i[r_\mu, r_\nu], \quad (23)$$

Since  $Q_H$  is not traceless, the operator  $F_{\mu\nu}^+$  can be divided into two parts:  $\hat{F}_{\mu\nu}^+$  and  $\text{Tr}(F_{\mu\nu}^+)$ . The operator  $\hat{F}_{\mu\nu}^+ = F_{\mu\nu}^+ - \frac{1}{3} \text{Tr}(F_{\mu\nu}^+)$  is traceless and transforms as the adjoint representation. Recall that the direct product  $3 \otimes \bar{3} = 1 \oplus 8$ . Therefore, there are two independent interaction terms in the  $\mathcal{O}(p^2)$  Lagrangians for the magnetic moments of the

doubly charmed baryons. The nonrelativistic Lagrangians corresponding to Eq. (21) are

$$\begin{aligned} \mathcal{L}^{(2)} = & a_1 \frac{-i}{4M_B} \bar{H} [S^\mu, S^\nu] \hat{F}_{\mu\nu}^+ H \\ & + a_2 \frac{-i}{4M_B} \bar{H} [S^\mu, S^\nu] \text{Tr}(F_{\mu\nu}^+) H. \end{aligned} \quad (24)$$

We also need the second-order pseudoscalar meson and doubly charmed baryon interaction Lagrangians,

$$\hat{\mathcal{L}}_{\text{int}}^{(2)} = \frac{ig_{h1}}{4M_B} \bar{\Psi} \sigma^{\mu\nu} [u_\mu, u_\nu] \Psi + \frac{ig_{h2}}{4M_B} \bar{\Psi} \sigma^{\mu\nu} \{u_\mu, u_\nu\} \Psi, \quad (25)$$

where  $M_B$  is the nucleon mass and  $g_{h1, h2}$  are the coupling constants. Recall that for SU(3) group representations,

$$3 \otimes \bar{3} = 1 \oplus 8, \quad (26)$$

$$8 \otimes 8 = 1 \oplus 8_1 \oplus 8_2 \oplus 10 \oplus \bar{10} \oplus 27. \quad (27)$$

Both  $u_\mu$  and  $u_\nu$  transform as the adjoint representation. The two terms in Eq. (25) corresponding to the product of  $u_\mu$  and  $u_\nu$  belong to the  $8_1$  and  $8_2$  flavor representations, respectively. The  $g_{h2}$  term vanishes because of the anti-symmetric Lorentz structure. Thus, there is only one linearly independent LEC,  $g_{h1}$ , which contributes to the present investigations of the doubly charmed baryon magnetic moments up to  $\mathcal{O}(p^4)$ . The second-order pseudoscalar meson and baryon nonrelativistic Lagrangians read

$$\hat{\mathcal{L}}_{\text{int}}^{(2)} = \frac{g_{h1}}{2M_B} \bar{H} [S^\mu, S^\nu] [u_\mu, u_\nu] H. \quad (28)$$

The above Lagrangians contribute to the doubly charmed baryon magnetic moments in Fig. 2(e).

### C. The higher-order chiral Lagrangians

To calculate the  $\mathcal{O}(p^3)$  magnetic moments at the tree level, we also need the  $\mathcal{O}(p^4)$  electromagnetic chiral Lagrangians. The possible flavor structures are listed in Table I, where  $\chi^+ = \text{diag}(0, 0, 1)$  at the leading order. Recalling the flavor representation in Eqs. (26) and (27), since both  $F_{\mu\nu}^+$  and  $\chi^+$  are diagonal, the  $[\hat{F}_{\mu\nu}^+, \hat{\chi}_+]$  term vanishes. Meanwhile, the  $\text{Tr}(F_{\mu\nu}^+) \text{Tr}(\chi_+)$  and  $\text{Tr}(F_{\mu\nu}^+) \hat{\chi}_+$  terms can be absorbed into Eq. (21) by renormalizing the LECs  $a_1$  and  $a_2$ . Thus, the independent  $\mathcal{O}(p^4)$  Lagrangians read

TABLE I. The possible flavor structures of  $\mathcal{O}(p^4)$  Lagrangians that contribute to the magnetic moments.

Group representation	$1 \otimes 1 \rightarrow 1$	$1 \otimes 8 \rightarrow 8$	$8 \otimes 1 \rightarrow 8$	$8 \otimes 8 \rightarrow 1$	$8 \otimes 8 \rightarrow 8_1$	$8 \otimes 8 \rightarrow 8_2$
Flavor structure	$\text{Tr}(F_{\mu\nu}^+) \text{Tr}(\chi_+)$	$\text{Tr}(F_{\mu\nu}^+) \hat{\chi}_+$	$\hat{F}_{\mu\nu}^+ \text{Tr}(\chi_+)$	$\text{Tr}(\hat{F}_{\mu\nu}^+ \hat{\chi}_+)$	$[\hat{F}_{\mu\nu}^+, \hat{\chi}_+]$	$\{\hat{F}_{\mu\nu}^+, \hat{\chi}_+\}$

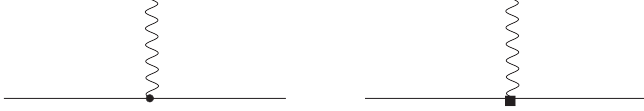


FIG. 1. The  $\mathcal{O}(p^2)$  and  $\mathcal{O}(p^4)$  tree-level diagrams, where the doubly charmed baryon is denoted by the solid line. The left solid dot and the right black square represent second- and fourth-order couplings, respectively.

$$\begin{aligned} \mathcal{L}^{(4)} = & \frac{d_1}{8M_B} \bar{\Psi} \text{Tr}(F_{\mu\nu}^+) \hat{\chi}^+ \sigma^{\mu\nu} \Psi \\ & + \frac{d_2}{8M_B} \bar{\Psi} \text{Tr}(\hat{F}_{\mu\nu}^+ \hat{\chi}^+) \sigma^{\mu\nu} \Psi + \frac{d_3}{8M_B} \bar{\Psi} \{ \hat{F}_{\mu\nu}^+, \hat{\chi}^+ \} \sigma^{\mu\nu} \Psi. \end{aligned} \quad (29)$$

Their nonrelativistic forms are

$$\begin{aligned} \mathcal{L}^{(4)} = & d_1 \frac{-i}{4M_B} \bar{H} [S^\mu, S^\nu] H \text{Tr}(F_{\mu\nu}^+) \hat{\chi}^+ \\ & + d_2 \frac{-i}{4M_B} \bar{H} [S^\mu, S^\nu] H \text{Tr}(\hat{F}_{\mu\nu}^+ \hat{\chi}^+) \\ & + d_3 \frac{-i}{4M_B} \bar{H} [S^\mu, S^\nu] H \{ \hat{F}_{\mu\nu}^+, \hat{\chi}^+ \}. \end{aligned} \quad (30)$$

#### IV. FORMALISM UP TO THE ONE-LOOP LEVEL

We follow the standard power-counting scheme as in Ref. [59]. The chiral order  $D_\chi$  is given by [60]

$$D_\chi = 4N_L - 2I_M - I_B + \sum_n nN_n, \quad (31)$$

where  $N_L$  is the number of loops,  $I_M$  is the number of the internal pion lines,  $I_B$  is the number of the internal baryon lines, and  $N_n$  is the number of the vertices from the  $n$ th-order Lagrangians. The chiral order of the magnetic moments  $\mu_H$  is  $(D_\chi - 1)$  based on Eq. (7).

We assume exact isospin symmetry with  $m_u = m_d$  throughout this work. The tree-level Lagrangians in Eqs. (24) and (30) contribute to the doubly charmed baryon magnetic moments at  $\mathcal{O}(p^1)$  and  $\mathcal{O}(p^3)$ , as shown in Fig. 1. The Clebsch-Gordan coefficients for the various doubly

charmed baryons are collected in Table II. All doubly charmed baryon magnetic moments are given in terms of  $a_1$ ,  $a_2$ ,  $d_1$ ,  $d_2$ , and  $d_3$ .

There are six Feynman diagrams that contribute to the doubly charmed baryon magnetic moments at the one-loop level, as shown in Fig. 2. Figures 2(a) and 2(c) contribute to the magnetic moments at  $\mathcal{O}(p^2)$ , while the other diagrams contribute at  $\mathcal{O}(p^3)$ . All the vertices represented by dots in these diagrams come from leading-order Lagrangians, while all the vertices represented by solid dots come from the  $\mathcal{O}(p^2)$  Lagrangians. In Fig. 2(a), the meson vertex is from the leading-order meson and baryon interaction Lagrangian in Eq. (20) and the photon vertex is from the leading-order pure meson Lagrangian in Eq. (14). In Fig. 2(b), the photon-meson-baryon vertex is from the  $\mathcal{O}(p^2)$  interaction terms in Eq. (24). In Fig. 2(c), the two vertices are from the strong interaction terms and seagull terms in Eq. (20), respectively. In Fig. 2(d), the meson vertex is from the strong interaction terms in Eq. (20), while the photon vertex is from the  $\mathcal{O}(p^2)$  interaction terms in Eq. (24). In Fig. 2(e), the meson-baryon vertex is from the second-order pseudoscalar meson and baryon Lagrangian in Eq. (28), while the photon vertex is also from the meson photon interaction term Eq. (24). In Fig. 2(f), the meson vertex is from the strong interaction terms, while the photon vertex is from the  $\mathcal{O}(p^2)$  in Eq. (24).

Figure 2(c) vanishes in the heavy-baryon-mass limit. In particular,

$$J_c \propto \int \frac{d^d l}{(2\pi)^d} \frac{i}{l^2 - m^2 + i\epsilon} (S \cdot l) \frac{i}{v \cdot l + i\epsilon} S^\mu \propto S \cdot v = 0. \quad (32)$$

In other words, Fig. 2(c) does not contribute to the magnetic moments in the leading order of the heavy baryon expansion. Figure 2(f) indicates the corrections from the wave-function renormalization.

Summing all the contributions to the doubly charmed baryon magnetic moments in Fig. 2, the leading- and next-to-leading-order loop corrections can be expressed as

$$\mu_H^{(2,\text{loop})} = - \sum_{\phi=\pi,K} \frac{\tilde{g}_A^2 m_\phi M_N \beta_a^\phi}{64\pi f_\phi^2}, \quad (33)$$

TABLE II. The doubly charmed baryon magnetic moments to the next-to-next-to-leading order (in units of  $\mu_N$ ).

Baryons	$\mathcal{O}(p^1)$ tree	$\mathcal{O}(p^2)$ loop	$\mathcal{O}(p^3)$ tree	$\mathcal{O}(p^3)$ loop
$\Xi_{cc}^{++}$	$\frac{2}{3}a_1 + 4a_2$	$-0.51\tilde{g}_A^2$	$-\frac{4}{3}d_1 - \frac{1}{3}d_2 - \frac{4}{9}d_3$	$0.15a_1 + 0.21a_2 - 0.27g_{h1}$
$\Xi_{cc}^+$	$-\frac{1}{3}a_1 + 4a_2$	$0.15\tilde{g}_A^2$	$-\frac{4}{3}d_1 - \frac{1}{3}d_2 + \frac{2}{9}d_3$	$-0.05a_1 + 0.21a_2 + 0.06g_{h1}$
$\Omega_{cc}^+$	$-\frac{1}{3}a_1 + 4a_2$	$0.36\tilde{g}_A^2$	$\frac{8}{3}d_1 - \frac{1}{3}d_2 - \frac{4}{9}d_3$	$-0.12a_1 + 0.36a_2 + 0.21g_{h1}$

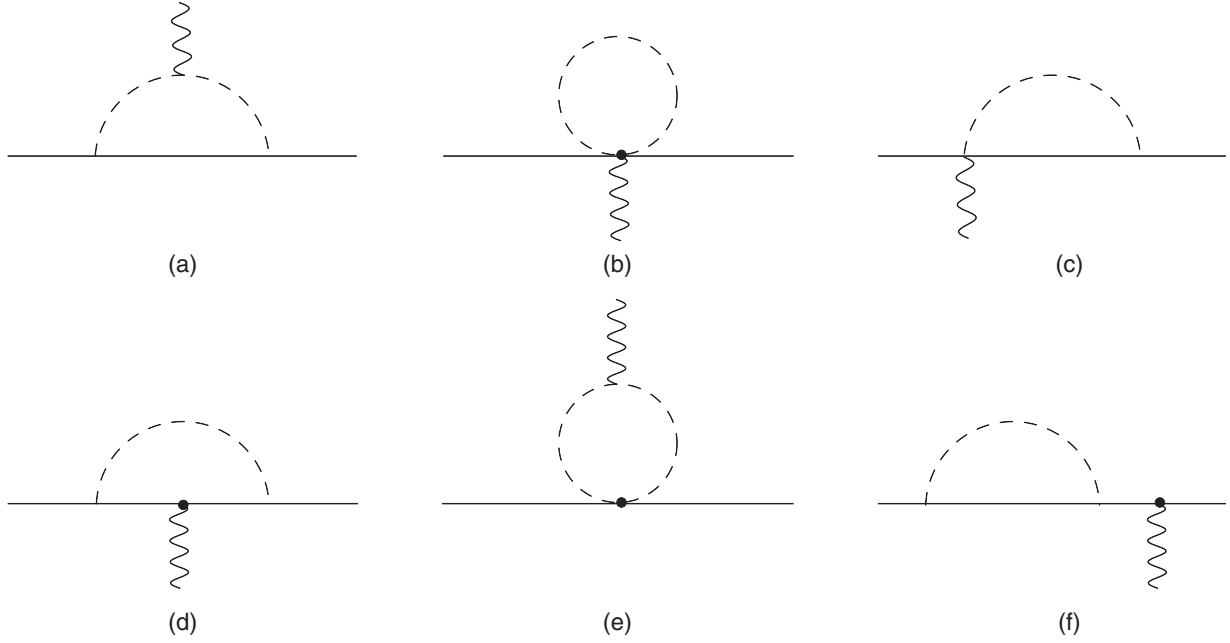


FIG. 2. The one-loop diagrams, where the doubly charmed baryon is denoted by the solid line. The dashed and wiggly lines represent the pseudoscalar meson and photon, respectively. The solid dots represent  $\mathcal{O}(p^2)$  vertices. Other vertices are leading order.

$$\begin{aligned} \mu_H^{(3,\text{loop})} = & \sum_{\phi=\pi,K} \left[ \frac{\beta_b^\phi m_\phi^2 \ln \frac{m_\phi^2}{\lambda^2}}{128\pi^2 f_\phi^2} + \frac{\beta_e^\phi m_\phi^2 \ln \frac{m_\phi^2}{\lambda^2}}{16\pi^2 f_\phi^2} \right] \\ & + \sum_{\phi=\pi,K,\eta} \left[ \frac{-\beta_d^\phi \tilde{g}_A^2 m_\phi^2}{512\pi^2 f_\phi^2} \left( \ln \frac{m_\phi^2}{\lambda^2} - 2 \right) \right. \\ & \left. + \frac{-3\beta_f^\phi \tilde{g}_A^2 m_\phi^2 \ln \frac{m_\phi^2}{\lambda^2}}{256\pi^2 f_\phi^2} \right], \end{aligned} \quad (34)$$

where  $\lambda = 4\pi f_\pi$  is the renormalization scale. Here, we use the number  $n$  within the parentheses in the superscript of  $X^{(n,\dots)}$  to indicate the chiral order of  $X$ .  $\beta_{a-f}^\phi$  arise from the corresponding diagrams in Fig. 2. We collect their explicit expressions in Tables VIII and IX in the Appendix.

With the low-energy counterterms and loop contributions (33)–(34), we obtain the magnetic moments,

$$\mu_H = \{\mu_H^{(1)}\} + \{\mu_H^{(2,\text{loop})}\} + \{\mu_H^{(3,\text{tree})} + \mu_H^{(3,\text{loop})}\}, \quad (35)$$

where  $\mu_H^{(1)}$  and  $\mu_H^{(3,\text{tree})}$  are the tree-level magnetic moments from Eqs. (24) and (30).

## V. NUMERICAL RESULTS AND DISCUSSIONS

There is currently no experimental data on the doubly charmed baryon magnetic moments. We do not have any experimental inputs to fit the LECs. In this paper, we use the quark model to estimate the leading-order low-energy constants. At the leading order  $\mathcal{O}(p^1)$ , there are two

unknown LECs:  $a_{1,2}$ . The charge matrix  $Q_H$  is not traceless, which is different from that in the case of the light baryons. Notice that the  $a_1$  parts are proportional to the light quark charge within the doubly charmed baryon. The  $a_2$  parts are the same for the three doubly charmed baryons and arise solely from the two charm quarks.

At the quark level, the flavor and spin wave function of  $\Xi_{cc}^{++}$  reads

$$\begin{aligned} |\Xi_{cc}^{++}; \uparrow\rangle = & \frac{1}{3\sqrt{2}} (2|c\uparrow c\uparrow u\downarrow\rangle - |c\uparrow c\downarrow u\uparrow\rangle - |c\downarrow c\uparrow u\uparrow\rangle \\ & + 2|c\uparrow u\downarrow c\uparrow\rangle - |c\downarrow u\uparrow c\uparrow\rangle \\ & - |c\downarrow u\downarrow c\downarrow\rangle + 2|u\downarrow c\uparrow c\uparrow\rangle \\ & - |u\downarrow c\downarrow c\downarrow\rangle - |u\uparrow c\downarrow c\uparrow\rangle), \end{aligned} \quad (36)$$

where the arrows denote the third components of the spin. Replacing the  $u$  quark by the  $d$  and  $s$  quarks, we get the wave functions of  $\Xi_{cc}^+$  and  $\Omega_{cc}^+$ , respectively. The magnetic moments of the doubly charmed baryons in the quark model are the matrix elements of the following operator in Eq. (36):

$$\vec{\mu} = \sum_i \mu_i \vec{\sigma}^i, \quad (37)$$

where  $\mu_i$  is the magnetic moment of the quark,

$$\mu_i = \frac{e_i}{2m_i}, \quad i = u, d, s. \quad (38)$$

We adopt the values  $m_u = m_d = 336$  MeV,  $m_s = 540$  MeV, and  $m_c = 1660$  MeV as the constituent quark

TABLE III. The doubly charmed baryon magnetic moments when the chiral expansion is truncated at  $\mathcal{O}(p^1)$  and  $\mathcal{O}(p^2)$ , respectively (in units of  $\mu_N$ ).

Baryons	$\mathcal{O}(p^1)$	$\mathcal{O}(p^2)$ loop	$\mathcal{O}(p^2)$ total
$\Xi_{cc}^{++}$	$\frac{4}{3}\mu_c - \frac{1}{3}\mu_u = -0.12$	-0.13	-0.25
$\Xi_{cc}^+$	$\frac{4}{3}\mu_c - \frac{1}{3}\mu_d = 0.81$	0.04	0.85
$\Omega_{cc}^+$	$\frac{4}{3}\mu_c - \frac{1}{3}\mu_s = 0.69$	0.09	0.78

masses and give the results in the second column in Table III. The light quark magnetic moments contribute to the LEC  $a_1$ , which are proportional to the light quark charge. The heavy quark magnetic moments contribute to the LEC  $a_2$ , which are the same for the three doubly charmed baryons. The magnetic moments of the three doubly charmed baryons are given in the second column in Table III.

Up to  $\mathcal{O}(p^2)$ , we need to include both the leading tree-level magnetic moments and the  $\mathcal{O}(p^2)$  loop corrections. At this order, there exists only one new LEC  $\tilde{g}_A$ . We also use the quark model to estimate  $\tilde{g}_A$ . Considering the  $\pi^0$  coupling at the hadron level,

$$\mathcal{L}_{\Xi_{cc}^{++}\Xi_{cc}^{++}\pi^0} = -\frac{1}{2F_0} \frac{\tilde{g}_A}{2} \bar{\Xi}_{cc}^{++} \gamma^\mu \gamma_5 \partial_\mu \pi^0 \Xi_{cc}^{++}. \quad (39)$$

At the quark level, the  $\pi^0$  quark interaction reads

$$\mathcal{L}_{\text{quark}} = \frac{1}{2} g_0 \bar{\Psi}_q \gamma^\mu \gamma_5 \partial_\mu \pi^0 \Psi_q. \quad (40)$$

With the help of the flavor wave functions of  $\Xi_{cc}^{++}$ , we obtain the matrix elements at the hadron level,

$$\left\langle \Xi_{cc}^{++}, s = \frac{1}{2} \left| i \mathcal{L}_{\Xi_{cc}^{++}\Xi_{cc}^{++}\pi^0} \right| \Xi_{cc}^{++}, s = \frac{1}{2}; \pi^0 \right\rangle \sim -\frac{1}{2F_0} \frac{\tilde{g}_A}{2} q_3, \quad (41)$$

and at the quark level,

$$\left\langle \Xi_{cc}^{++}, s = \frac{1}{2} \left| i \mathcal{L}_{\text{quark}} \right| \Xi_{cc}^{++}, s = \frac{1}{2}; \pi^0 \right\rangle \sim -\frac{1}{6} g_0 q_3. \quad (42)$$

After comparison with the axial charge of the nucleon,

$$\frac{\frac{1}{2} \tilde{g}_A}{\frac{-1}{6} g_0} = \frac{\frac{1}{2} g_A}{\frac{5}{6} g_0}, \quad (43)$$

one obtains  $\tilde{g}_A = -\frac{2}{5} g_A = -0.5$ . Thus, we obtain the numerical results of  $\mathcal{O}(p^2)$  chiral loop corrections, which are shown in the third column in Table III. We list the numerical results of the  $\mathcal{O}(p^2)$  magnetic moments of the three doubly charmed baryons in the fourth column in Table III. We also compare the numerical results of the

TABLE IV. The doubly bottom baryon magnetic moments ( $bbq$ ) to the next-to-leading order (in units of  $\mu_N$ ).

Baryons	$\mathcal{O}(p^1)$ tree	$\mathcal{O}(p^2)$ loop	Total
$\Xi_{bb}^0$	$\frac{4}{3}\mu_b - \frac{1}{3}\mu_u = -0.71$	-0.13	-0.84
$\Xi_{bb}^-$	$\frac{4}{3}\mu_b - \frac{1}{3}\mu_d = 0.22$	0.04	0.26
$\Omega_{bb}^-$	$\frac{4}{3}\mu_b - \frac{1}{3}\mu_s = 0.10$	0.09	0.19

magnetic moments when the chiral expansions are truncated at  $\mathcal{O}(p^1)$  and  $\mathcal{O}(p^2)$ , respectively, in Table III.

Up to  $\mathcal{O}(p^3)$ , there are six unknown LECs:  $a_{1,2}$ ,  $g_{h1}$ ,  $d_{1,2,3}$ . Unfortunately, we are not able to present numerical results since it is impossible to fix all of these LECs with the available experimental information. We present our analytical results in Eqs. (33) and (34) and Table II. Our analytical results may be useful to the possible chiral extrapolation of the lattice simulations of the doubly charmed baryon electromagnetic properties.

We also calculate the magnetic moments of the other doubly heavy baryons. At the quark level, the flavor and spin wave functions of the doubly bottom baryons are the same as those of the doubly charmed baryons after replacing the  $c$  quarks by  $b$  quarks. After the similar calculations of Eqs. (36)–(43), one obtains the axial charge of doubly bottom baryons  $\tilde{g}_A(bbq) = \frac{2}{5} g_A$  and the tree-level magnetic moments of the three doubly bottom baryons, which are shown in the second column in Table IV. We collect the numerical results of doubly bottom baryon magnetic moments to next-to-leading order in Table IV.

We also calculate the magnetic moments of the doubly heavy baryons containing a light quark, a charm quark, and a bottom quark. We refer to the charm quark and the bottom quark as a diquark. There are two different multiplets of the

TABLE V. The magnetic moments of doubly heavy baryons ( $\{bc\}q$ ) to the next-to-leading order (in units of  $\mu_N$ ).

Baryons	$\mathcal{O}(p^1)$ tree	$\mathcal{O}(p^2)$ loop	Total
$\Xi_{\{bc\}q}^+$	$\frac{1}{3}(2\mu_b + 2\mu_c - \mu_u) = -0.41$	-0.13	-0.54
$\Xi_{\{bc\}q}^0$	$\frac{1}{3}(2\mu_b + 2\mu_c - \mu_d) = 0.52$	0.04	0.56
$\Omega_{\{bc\}u}^0$	$\frac{1}{3}(2\mu_b + 2\mu_c - \mu_s) = 0.40$	0.09	0.49

TABLE VI. The magnetic moments of doubly heavy baryons ( $[bc]q$ ) to the next-to-leading order (in units of  $\mu_N$ ).

Baryons	$\mathcal{O}(p^1)$ tree	$\mathcal{O}(p^2)$ loop	Total
$\Xi_{[bc]q}^+$	$\mu_u = 1.86$	-1.17	0.69
$\Xi_{[bc]q}^0$	$\mu_d = -0.93$	0.34	-0.59
$\Omega_{[bc]u}^0$	$\mu_s = -0.58$	0.82	0.24

doubly heavy baryons. The symmetric diquark ( $\{bc\}$ ) has spin 1, while the antisymmetric diquark ( $[bc]$ ) has spin 0.

At the quark level, the flavor and spin wave function of the ( $\{bc\}q$ ) baryons reads

$$|\{bc\}q; \uparrow\rangle = \frac{1}{\sqrt{2}}(|cbq\rangle + |bcq\rangle) \otimes \frac{1}{\sqrt{6}}(2|\uparrow\uparrow\downarrow\rangle - |\uparrow\downarrow\uparrow\rangle - |\downarrow\uparrow\uparrow\rangle), \quad (44)$$

while the flavor and spin wave function of the ( $[bc]q$ ) baryons reads

$$|[bc]q; \uparrow\rangle = \frac{1}{\sqrt{2}}(|cbq\rangle - |bcq\rangle) \otimes \frac{1}{\sqrt{2}}(|\uparrow\downarrow\uparrow\rangle - |\downarrow\uparrow\uparrow\rangle). \quad (45)$$

After similar calculations, one obtains the axial charge of the  $\{bc\}q$  baryons  $\tilde{g}_A(\{bc\}q) = -\frac{2}{5}g_A$  and the axial charge of the  $[bc]q$  baryons  $\tilde{g}_A([bc]q) = \frac{6}{5}g_A$ . We collect the tree-level magnetic moments of the  $\{bc\}q$  baryons in the second column in Table V and the tree-level magnetic moments of the three  $[bc]q$  baryons in the second column in Table VI. We collect the numerical results of the  $\{bc\}q$  and  $[bc]q$  baryon magnetic moments to next-to-leading order in the fourth column in Table V and Table VI, respectively.

## VI. CONCLUSIONS

The discovery of  $\Xi_{cc}^{++}$  inspired heated theoretical investigation of the doubly charmed baryons. The doubly charmed baryons are so special that the chiral dynamics is dominated by the single light quark. The electromagnetic property of the doubly charmed baryons encodes crucial information about their inner structure. In this work, we have performed systematical calculations of the chiral corrections to the magnetic moments of doubly charmed baryons up to the next-to-next-to-leading order in the framework of heavy baryon chiral perturbation theory. We used the quark model to estimate the low-energy constants and present the numerical results up to next-to-leading order:  $\mu_{\Xi_{cc}^{++}} = -0.25\mu_N$ ,  $\mu_{\Xi_{cc}^+} = 0.85\mu_N$ ,  $\mu_{\Omega_{cc}^+} = 0.78\mu_N$ .

From Table III, the magnetic moments of  $\Xi_{cc}^+$  and  $\Omega_{cc}^+$  are dominated by the leading-order term, while the chiral corrections are quite small. To be specific, the numerical values of the  $\mathcal{O}(p^1)$  magnetic moments of  $\Xi_{cc}^+$  and  $\Omega_{cc}^+$  are enhanced since the charge of the down and strange quarks is  $-\frac{1}{3}$  while the charm quark charge is  $+\frac{2}{3}$ . Only the  $\pi^+$  meson contributes to the chiral correction to  $\mu_{\Xi_{cc}^+}$  at  $\mathcal{O}(p^2)$ , while only  $K^+$  contributes to  $\mu_{\Omega_{cc}^+}$  at this order.

For comparison, the up and charm quark contributions to the  $\mathcal{O}(p^1)$  magnetic moment of  $\Xi_{cc}^{++}$  are destructive. Such

an accidental strong cancellation renders the leading-order magnetic moment of  $\Xi_{cc}^{++}$  much smaller than those of its partner states. In contrast, both the  $\pi^+$  and  $K^+$  mesons contribute to the chiral corrections to  $\mu_{\Xi_{cc}^{++}}$  at  $\mathcal{O}(p^2)$ . In other words, the leading-order magnetic moment of  $\Xi_{cc}^{++}$  is reduced while the loop correction is enhanced. As a result, the loop correction is numerically very important and even slightly larger than the leading-order term. Such a unique feature can be exposed by future lattice QCD simulations.

In Table VII, we compare our results obtained in HBChPT with those from other model calculations, such as the quark model [41], relativistic three-quark model [43], nonrelativistic quark model in the Faddeev approach [8], relativistic quark model [42], Skyrmon description [48], confining logarithmic potential [47], MIT bag model [45], nonrelativistic quark model [49], and lattice QCD. All of these approaches lead to roughly consistent results.

As by-products, we have also calculated the magnetic moments of the other doubly heavy baryons, including the  $bbq$  baryons, the  $\{bc\}q$  baryons, and the  $[bc]q$  baryons. In particular, the magnetic moments of the  $[bc]q$  baryons are quite interesting as their magnetic moments totally arise from the light quarks, as shown in Table VI.

We hope our calculation may be useful for future experimental measurements. As there are several unknown LECs up to next-to-next-to-leading order, we are looking forward to further progresses in both theory and experiment so that we can check the chiral expansion convergence of the three doubly charmed baryons. Our results may be useful for future experimental measurements of the magnetic moments. Our analytical results may also be useful for the possible chiral extrapolation of the lattice simulations.

TABLE VII. Comparison of the decuplet to octet baryon transition magnetic moments in the literature, including the quark model (QM) [41], relativistic three-quark model (RTQM) [43], nonrelativistic quark model in the Faddeev approach (NQM) [8], relativistic quark model (RQM) [42], Skyrmon description [48], confining logarithmic potential (CLP) [47], MIT bag model [45], nonrelativistic quark model (NQM) [49], and lattice QCD (LQCD) [51] (in units of  $\mu_N$ ).

Baryons	$\Xi_{cc}^{++}$	$\Xi_{cc}^+$	$\Omega_{cc}^+$
QM [41]	-0.124	0.806	0.688
RTQM [43]	0.13	0.72	0.67
NRQM [8]	-0.206	0.784	0.635
RQM [42]	-0.10	0.86	0.72
Skyrmon [48]	-0.47	0.98	0.59
CLP [47]	-0.154	0.778	0.657
MIT bag model [45]	0.17	0.86	0.84
NQM [49]	-0.208	0.785	0.635
LQCD [51]	—	0.425	0.413
This work	-0.25	0.85	0.78

## ACKNOWLEDGMENTS

H. S. L. is very grateful to X. L. Chen and W. Z. Deng for very helpful discussions. This project is supported by the National Natural Science Foundation of China under Grants No. 11575008, 11621131001 and 973 program. This work is also supported by the Fundamental Research Funds for the Central Universities of Lanzhou University under Grants No. 223000–862637.

## APPENDIX: COEFFICIENTS OF THE LOOP CORRECTIONS

In this appendix, we collect the explicit formulae for the chiral expansion of the doubly charmed baryon magnetic moments in Tables VIII and IX.

TABLE VIII. The coefficients of the loop corrections to the doubly charmed baryon magnetic moments from Figs. 2(a), 2(b), and 2(d).

Baryons	$\beta_a^\pi$	$\beta_a^K$	$\beta_b^\pi$	$\beta_b^K$	$\beta_d^\pi$	$\beta_d^K$	$\beta_d^\eta$
$\Xi_{cc}^{++}$	2	2	$-4a_1$	$-4a_1$	$24a_2$	$-\frac{4}{3}a_1 + 16a_2$	$\frac{4}{9}(a_1 + 6a_2)$
$\Xi_{cc}^+$	-2	0	$4a_1$	0	$2a_1 + 24a_2$	$-\frac{4}{3}a_1 + 16a_2$	$\frac{2}{9}(-a_1 + 12a_2)$
$\Omega_{cc}^+$	0	-2	0	$4a_1$	0	$\frac{4}{3}(a_1 + 24a_2)$	$-\frac{8}{9}(a_1 - 12a_2)$

TABLE IX. The coefficients of the loop corrections to the doubly charmed baryon magnetic moments from Figs. 2(e) and 2(f).

Baryons	$\beta_e^\pi$	$\beta_e^K$	$\beta_f^\pi$	$\beta_f^K$	$\beta_f^\eta$
$\Xi_{cc}^{++}$	$g_{h1}$	$g_{h1}$	$2(a_1 + 6a_2)$	$\frac{4}{3}(a_1 + 6a_2)$	$\frac{2}{9}(a_1 + 6a_2)$
$\Xi_{cc}^+$	$-g_{h1}$	0	$-a_1 + 12a_2$	$-\frac{2}{3}a_1 + 8a_2$	$-\frac{1}{9}a_1 + \frac{4}{3}a_2$
$\Omega_{cc}^+$	0	$-g_{h1}$	0	$-\frac{4}{3}a_1 + 16a_2$	$-\frac{4}{9}(a_1 - 12a_2)$

- 
- [1] M. Mattson *et al.* (SELEX Collaboration), *Phys. Rev. Lett.* **89**, 112001 (2002).
- [2] S. P. Ratti, *Nucl. Phys. B, Proc. Suppl.* **115**, 33 (2003).
- [3] B. Aubert *et al.* (BABAR Collaboration), *Phys. Rev. D* **74**, 011103 (2006).
- [4] R. Chistov *et al.* (Belle Collaboration), *Phys. Rev. Lett.* **97**, 162001 (2006).
- [5] R. Aaij *et al.* (LHCb Collaboration), *Phys. Rev. Lett.* **119**, 112001 (2017).
- [6] E. Bagan, M. Chabab, and S. Narison, *Phys. Lett. B* **306**, 350 (1993).
- [7] R. Roncaglia, D. B. Lichtenberg, and E. Predazzi, *Phys. Rev. D* **52**, 1722 (1995).
- [8] B. Silvestre-Brac, *Few-Body Syst.* **20**, 1 (1996).
- [9] D. Ebert, R. N. Faustov, V. O. Galkin, A. P. Martynenko, and V. A. Saleev, *Z. Phys. C* **76**, 111 (1997).
- [10] S. P. Tong, Y. B. Ding, X. H. Guo, H. Y. Jin, X. Q. Li, P. N. Shen, and R. Zhang, *Phys. Rev. D* **62**, 054024 (2000).
- [11] C. Itoh, T. Minamikawa, K. Miura, and T. Watanabe, *Phys. Rev. D* **61**, 057502 (2000).
- [12] S. S. Gershtein, V. V. Kiselev, A. K. Likhoded, and A. I. Onishchenko, *Phys. Rev. D* **62**, 054021 (2000).
- [13] V. V. Kiselev and A. K. Likhoded, *Usp. Fiz. Nauk* **172**, 497 (2002) [*Phys. Usp.* **45**, 455 (2002)].
- [14] V. V. Kiselev, A. K. Likhoded, O. N. Pakhomova, and V. A. Saleev, *Phys. Rev. D* **66**, 034030 (2002).
- [15] I. M. Narodetskii and M. A. Trusov, *Yad. Fiz.* **65**, 949 (2002) [*Phys. At. Nucl.* **65**, 917 (2002)].
- [16] R. Lewis, N. Mathur, and R. M. Woloshyn, *Phys. Rev. D* **64**, 094509 (2001).
- [17] A. Faessler, T. Gutsche, M. A. Ivanov, J. G. Korner, and V. E. Lyubovitskij, *Phys. Lett. B* **518**, 55 (2001).
- [18] D. Ebert, R. N. Faustov, V. O. Galkin, and A. P. Martynenko, *Phys. Rev. D* **66**, 014008 (2002).
- [19] N. Mathur, R. Lewis, and R. M. Woloshyn, *Phys. Rev. D* **66**, 014502 (2002).
- [20] J. M. Flynn, F. Mescia, and A. S. B. Tariq (UKQCD Collaboration), *J. High Energy Phys.* **07** (2003) 066.
- [21] J. Vijande, H. Garcilazo, A. Valcarce, and F. Fernandez, *Phys. Rev. D* **70**, 054022 (2004).
- [22] T. W. Chiu and T. H. Hsieh, *Nucl. Phys.* **A755**, 471 (2005).
- [23] S. Migura, D. Merten, B. Metsch, and H. R. Petry, *Eur. Phys. J. A* **28**, 41 (2006).
- [24] C. Albertus, E. Hernandez, J. Nieves, and J. M. Verde-Velasco, *Eur. Phys. J. A* **32**, 183 (2007); **36**, 119(E) (2008).

- [25] X. Liu, H. X. Chen, Y. R. Liu, A. Hosaka, and S. L. Zhu, *Phys. Rev. D* **77**, 014031 (2008).
- [26] W. Roberts and M. Pervin, *Int. J. Mod. Phys. A* **23**, 2817 (2008).
- [27] A. Valcarce, H. Garcilazo, and J. Vijande, *Eur. Phys. J. A* **37**, 217 (2008).
- [28] L. Liu, H. W. Lin, K. Orginos, and A. Walker-Loud, *Phys. Rev. D* **81**, 094505 (2010).
- [29] Y. Namekawa (PACS-CS Collaboration), *Proc. Sci.*, LATTICE2012 (2012) 139.
- [30] C. Alexandrou, J. Carbonell, D. Christaras, V. Drach, M. Gravina, and M. Papinutto, *Phys. Rev. D* **86**, 114501 (2012).
- [31] T. M. Aliev, K. Azizi, and M. Savci, *Nucl. Phys.* **A895**, 59 (2012).
- [32] T. M. Aliev, K. Azizi, and M. Savci, *J. Phys. G* **40**, 065003 (2013).
- [33] Y. Namekawa *et al.* (PACS-CS Collaboration), *Phys. Rev. D* **87**, 094512 (2013).
- [34] Z. F. Sun, Z. W. Liu, X. Liu, and S. L. Zhu, *Phys. Rev. D* **91**, 094030 (2015).
- [35] H. X. Chen, W. Chen, Q. Mao, A. Hosaka, X. Liu, and S. L. Zhu, *Phys. Rev. D* **91**, 054034 (2015).
- [36] Z. F. Sun and M. J. Vicente Vacas, *Phys. Rev. D* **93**, 094002 (2016).
- [37] Z. Shah, K. Thakkar, and A. K. Rai, *Eur. Phys. J. C* **76**, 530 (2016).
- [38] H. X. Chen, W. Chen, X. Liu, Y. R. Liu, and S. L. Zhu, *Rep. Prog. Phys.* **80**, 076201 (2017).
- [39] A. V. Kiselev, A. V. Berezhnoy, and A. K. Likhoded, [arXiv:1706.09181](https://arxiv.org/abs/1706.09181).
- [40] H. X. Chen, Q. Mao, W. Chen, X. Liu, and S. L. Zhu, *Phys. Rev. D* **96**, 031501 (2017).
- [41] D. B. Lichtenberg, *Phys. Rev. D* **15**, 345 (1977).
- [42] B. Julia-Diaz and D. O. Riska, *Nucl. Phys.* **A739**, 69 (2004).
- [43] A. Faessler, T. Gutsche, M. A. Ivanov, J. G. Korner, V. E. Lyubovitskij, D. Nicmorus, and K. Pumsa-ard, *Phys. Rev. D* **73**, 094013 (2006).
- [44] T. Branz, A. Faessler, T. Gutsche, M. A. Ivanov, J. G. Korner, V. E. Lyubovitskij, and B. Oexl, *Phys. Rev. D* **81**, 114036 (2010).
- [45] S. K. Bose and L. P. Singh, *Phys. Rev. D* **22**, 773 (1980).
- [46] A. Bernotas and V. Simonis, [arXiv:1209.2900](https://arxiv.org/abs/1209.2900).
- [47] S. N. Jena and D. P. Rath, *Phys. Rev. D* **34**, 196 (1986).
- [48] Y. s. Oh, D. P. Min, M. Rho, and N. N. Scoccola, *Nucl. Phys.* **A534**, 493 (1991).
- [49] B. Patel, A. K. Rai, and P. C. Vinodkumar, [arXiv:0803.0221](https://arxiv.org/abs/0803.0221).
- [50] K. U. Can, G. Erkol, B. Isildak, M. Oka, and T. T. Takahashi, *Phys. Lett. B* **726**, 703 (2013).
- [51] K. U. Can, G. Erkol, B. Isildak, M. Oka, and T. T. Takahashi, *J. High Energy Phys.* **05** (2014) 125.
- [52] S. Weinberg, *Physica A* **96**, 327 (1979).
- [53] E. E. Jenkins and A. V. Manohar, *Phys. Lett. B* **255**, 558 (1991).
- [54] E. E. Jenkins, M. E. Luke, A. V. Manohar, and M. J. Savage, *Phys. Lett. B* **302**, 482 (1993); **388**, 866(E) (1996).
- [55] V. Bernard, N. Kaiser, J. Kambor, and U. G. Meissner, *Nucl. Phys.* **B388**, 315 (1992).
- [56] V. Bernard, N. Kaiser, and U. G. Meissner, *Int. J. Mod. Phys. E* **04**, 193 (1995).
- [57] H. S. Li, Z. W. Liu, X. L. Chen, W. Z. Deng, and S. L. Zhu, *Phys. Rev. D* **95**, 076001 (2017).
- [58] S. Scherer, *Adv. Nucl. Phys.* **27**, 277 (2003).
- [59] H. S. Li, Z. W. Liu, X. L. Chen, W. Z. Deng, and S. L. Zhu, [arXiv:1706.06458](https://arxiv.org/abs/1706.06458).
- [60] G. Ecker, *Prog. Part. Nucl. Phys.* **35**, 1 (1995).